

Research Paper

Calcium Supplement by Tetracycline guided amorphous Calcium Carbonate potentiates Osteoblast promotion for Synergetic Osteoporosis Therapy

Jianwei Wang^{2*}, Shan Tao^{1*}, Xiangyu Jin¹, Yanqing Song¹, Wentao Zhou¹, Haiya Lou³, Rui Zhao³, Cheng Wang^{1,4}✉, Fuqiang Hu¹ and Hong Yuan¹✉

1. College of Pharmaceutical Science, Zhejiang University, 866 Yuhangtang Road, Hangzhou, 310058, China.
2. The Second Affiliated Hospital, School of Medicine, Zhejiang University, No. 88 Jiefang Road, Hangzhou, 310009, China.
3. Sir Run Run Shaw Hospital, School of Medicine, Zhejiang University, No. 3 Qingchun East Road, Hangzhou, 310016, China.
4. School of Pharmaceutical Engineering & Life Science, Changzhou University, Changzhou, 213164, China.

*These authors contributed equally to this work.

✉ Corresponding authors: E-mails: 11519016@zju.edu.cn (C. Wang); yuanhong70@zju.edu.cn (H. Yuan).

© The author(s). This is an open access article distributed under the terms of the Creative Commons Attribution License (<https://creativecommons.org/licenses/by/4.0/>). See <http://ivyspring.com/terms> for full terms and conditions.

Received: 2020.02.20; Accepted: 2020.06.01; Published: 2020.07.09

Abstract

Background: The calcium supplement is a clinically approved approach for osteoporosis therapy but usually requires a large dosage without targetability and with poor outcome. This modality is not fully explored in current osteoporosis therapy due to the lack of proper calcium supplement carrier.

Methods: In this study, we constructed a tetracycline (Tc) modified and simvastatin (Sim) loaded phospholipid-amorphous calcium carbonate (ACC) hybrid nanoparticle (Tc/ACC/Sim).

Results: The resulted Tc/ACC/Sim was able to enhance its accumulation at the osteoporosis site. Most importantly, the combination of calcium supplement and Sim offered synergetic osteoblast promotion therapy of osteoporosis with advanced performance than non-targeted system or mono therapy.

Conclusion: This platform provides an alternative approach to stimulate bone formation by synergetic promotion of osteoblast differentiation using calcium supplement and Sim.

Key words: calcium supplement; osteoporosis; amorphous calcium carbonate; osteoblast promotion

Introduction

Osteoporosis is a common bone disease which can occur in any age as well as sex [1, 2]. It is characterized as the disruption of bone homeostasis and loss of bone tissue which result in fracture and skeletal pain [3]. The cause of osteoporosis remains unclear but clinical evidences have identified several beneficial treatments for osteoporosis, which include supplement of bisphosphonates, estrogen and related compounds, vitamin D and calcitonin [4]. In particular, the calcium supplement in combination with vitamin D is supposed to be a conventional strategy for osteoporosis therapy [5]. However, this approach usually requires relatively large dosage of calcium supplement and suffered from poor outcome

which might due the fact that most of the adopted calcium ions are excreted without precise targeting to the lesions [6]. Although nanomedicine employing advanced nanotechnology has shown beneficial effects on the reverse of osteoporosis [7-9], the calcium supplement modality for osteoporosis therapy is not fully explored in current osteoporosis therapies, which might due to the lack of proper calcium supplement carrier. Therefore, the development of osteoporosis targeted system might be challenging but highly desirable.

Our previous studies have revealed that amorphous calcium carbonate (ACC) as the unique form of calcium carbonate family usually exerts high

water solubility upon exposure in aqueous environment while at the same reserves the acid responsive nature of common calcium carbonates, which results in faster calcium release of ACC in acidic environments as compared to other calcium containing materials [10, 11]. In addition, it was generally recognized that the osteoclast activation is usually associated with the release of phosphate radicals, which gradually develops an acidic microenvironment within the osteoporosis lesions [12, 13]. As a result, in our opinion, if being properly modified, ACC might be a preferable calcium supplement for osteoporosis therapy.

Tetracycline (Tc) is a broad-spectrum antibiotic which is employed to cure bacterial infections [14]. However, in-depth study further reveals the preferable internalization of Tc into the bone, which possibly through a reaction that appears to occur directly between Tc and hydroxyapatite (HAP), the major constituent of bone tissue [15]. It has previously been reported that bone disease may produce local inflammation that lead to blood exposure of HAP [16], which offers the possibility for targeting therapy of osteoporosis. As expected, several previous studies have suggested the promising bone targeting of Tc modified nanoparticles for osteoporosis therapy, which offers the possibility of employing ACC in osteoporosis targeted calcium supplement [17, 18].

The bone morphogenetic proteins (BMPs)-Smad is one of the important regulatory signaling pathway responsible for the formation of bone [19]. It was well recognized that BMP, originated from the transforming growth factor (TGF)- β superfamily, plays an important role in the regulation of embryonic development [20]. Employing the Smad signaling pathway to transduce osteogenic signals into bone marrow mesenchymal stem cells (MMSC), BMP not only promotes the differentiation of osteoprogenitor cells into osteoblasts, but also activates MMSC to differentiate into chondrocytes and osteoblasts [21, 22]. Considering the fact that BMP down-regulation is usually observed in the progress of osteoporosis, accumulating evidences have revealed that simvastatin (Sim) can increase the expression of BMP-2 in osteoblasts and promotes the formation of new bone through the BMP-Smad signaling pathway [23, 24], which may be applied as a novel drug for the treatment of osteoporosis to break traditional methods of inhibiting osteoclast activity [4, 25].

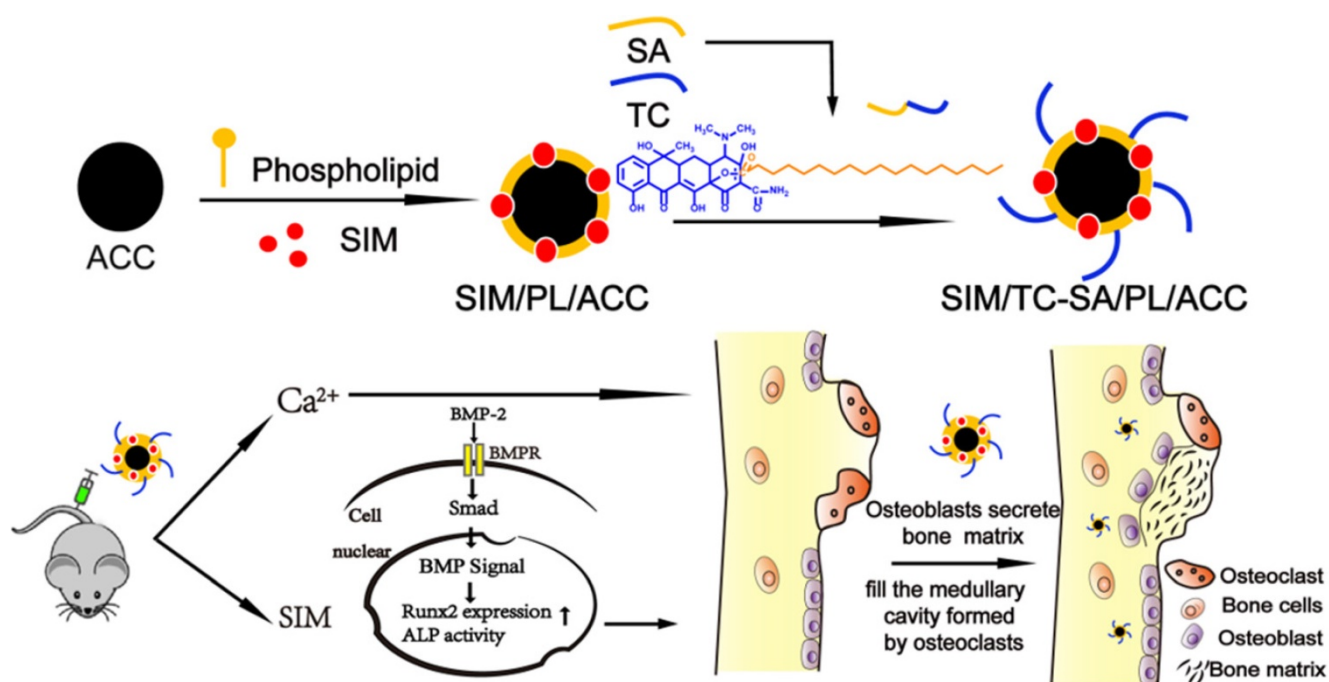
Herein our study, ACC nanoparticle was firstly synthesized as the core skeleton of the drug delivery system (DDS). Afterwards, the phospholipid (PL) was anchored on the surface of ACC to preserve the aqueous instability of ACC, during which the Tc

conjugated stearic acid (Tc-SA) was inserted and Sim was loaded into the PL layer of the nanoparticles at the same time (Scheme 1). The finally constructed Tc/ACC/Sim was characterized regarding its size distribution, morphology, zeta potential as well as cytotoxicity on MC3T3-E1 (clonal newborn mouse calvaria) cells. The osteoporosis targeted capability of Tc/ACC/Sim was further evaluated and the optimized drug administration dosage was explored. Finally, the *in vitro* and *in vivo* osteoporosis reversing efficacy of Tc/ACC/Sim were investigated to confirm the promising osteoporosis therapy using synergetic calcium supplement and osteoblast promotion strategy. Our results concluded that calcium supplement in combination of Sim activated BMP-2 in osteoblasts (through the BMP-Smad signaling pathway) was suggested to promote the formation of new bone to finally reverse the osteoporosis process in treated subjects.

Experimental Section

Materials

Calcium chloride (CaCl_2) and ammonium carbonate ($(\text{NH}_4)_2\text{CO}_3$) were obtained from Shanghai Chemical Reagent Co., Ltd. (Shanghai, China). Hydroxyapatite (HAP, melting point: 1650 °C; density: 3.16 g/cm³; water solubility: 0.4 ppm) was obtained from Sinopharm Chemical Reagent Co., Ltd. (Shanghai, China). Phospholipid (PL, extracted from the egg yolk with the purity of $\geq 90\%$, CAS: 93685-90-6) was purchased from A.V.T. Pharmaceutical Co., Ltd (Shanghai, China). Sim was obtained from Zhejiang Hisun Pharmaceutical Co., Ltd. (Zhejiang, China). Otcadecylamine (ODA), 4',6-Diamidino-2-phenylindole (DAPI), fluorescein isothiocyanate (FITC), stearic acid (SA), N,N'-disuccinimidyl carbonate (DSC), 1-(3-dimethylamino-propyl)-3-ethylcarbodiimide (EDC), 1-Hydroxybenzotriazole (HOBT), L-ascorbic acid, alizarin red S, β -glycerophosphate and 3-(4,5-dimethylthiazol-2-yl)-2,5-diphenyl-tetrazolium bromide (MTT) were obtained from Sigma (St.Louis, MO, USA). Poloxamer 188 was obtained from Shenyang Jiqi Pharmaceutical Co., Ltd. (China). The bicinchoninic acid (BCA) protein assay kit and alkaline phosphatase (ALP) test kit were obtained from the Solarbio (Beijing, China). Indocyanine green (ICG) was purchased from Molecular Probes (Eugene, OR, USA). Alpha-minimum essential medium (α MEM) was from Thermo-Fisher Scientific (Waltham, MA, USA). Other reagents otherwise stated were of analytical and from Shanghai Chemical Reagent Co., Ltd.



Scheme 1. A biological mechanism by which calcium supplement using ACC augments Sim mediated BMP-2-induced osteoblast differentiation is shown as Runx2 expression and ALP activity through the BMP-Smad signaling pathway.

Synthesis and characterization of Tetracycline stearic acid graft (Tc-SA)

Firstly, Tc-SA was synthesized by a simple esterification reaction between hydroxy group of Tc and carboxyl group of SA in the presence of EDC and HOBT. Briefly, SA (213 mg), EDC (216 mg) and HOBT (150 mg) at the mol ratio of 1:1.5:1.5 (SA: EDC: HOBT) were co-dissolved in 30 mL anhydrous DMF. The solution was stirred at 40°C with a mechanical stirring at 400 rpm for 30min to activate the carboxyl group of SA under the protection of nitrogen. Then, 10 mL anhydrous DMF containing 469 mg Tc (SA:Tc=1:1.3, mol:mol) was then added dropwise to the reaction solution. After 24 h of reaction under stirring at 40°C, Tc-SA was obtained, which was then dialyzed against distilled water for 48 h using a dialysis membrane bag (molecular cutoff = 7 kDa). After centrifugation at 4,000 rpm for 10 minutes and washed three times with the deionized water, final Tc-SA product was obtained, the structure of which was evaluated by ^1H NMR.

Preparation of fluorescein

We synthesized the fluorescent label ODA-FITC through a chemical grafting between the amino group of ODA and the isothiocyanate group of FITC according to our previous reported protocol [26]. Briefly, 28 mg of FITC and 20 mg of ODA were dissolved in 6 mL of ethanol and stirred at 50 °C for 24 h in the dark. After which, 50 mL of distilled water was added to precipitate ODA-FITC. The product was

washed three times with distilled water. In the end, the ODA-FITC was dried at room temperature and stored in the dark.

Preparation of blank PL/ACC and Sim-loaded PL/ACC (PL/ACC/Sim)

ACC was firstly synthesized with a vapor-diffusion method [27]. Briefly, 200 mg CaCl_2 was dissolved in 300 μl distilled water, which was added to a glass bottle containing 100 mL absolute ethanol. The glass bottle was subsequently covered by parafilm with several pores. The bottle was put in a desiccator along with two glass bottles containing 3 g of solid $(\text{NH}_4)_2\text{CO}_3$ at 35 °C. After vapor diffusion reaction for 1-2 days, the products were centrifuged (Allegra 64R, Beckman Coulter, USA, 15000 rpm, 10 min), rinsed several times and then re-dispersed in proper amount of absolute ethanol.

The ACC were then dispersed into ethanol containing PL (PL: ACC = 1, w/w) and 20% (w/w to PL) of Tc-SA (Tc/ACC) or not (PL/ACC). After stirring at 37 °C for 24 h, the mixture was ultrasonicated at 600 W for 20 cycles (20 KHz, 13 mm, work 2 s and stand 3 s) by a Lab ultrasonic cell pulverizer (JY92-II, Ningbo Scientz Biotechnology Co., Ltd, China) and then centrifuged at 3000 rpm for 10 min to remove unbounded free PL. The obtained supernatant was injected into water (1:9, ethanol : water ratio) under mechanical stirring. When preparing PL/ACC/Sim, Sim was added to the equivalent lipid component of blank PL/ACC (1:3

w/w, Sim : PL ratio). The other steps are the same as above.

Characterization of Tc/ACC/Sim

First, the carrier concentration of ACC, Tc/ACC, PL/ACC/Sim and Tc/ACC/Sim were diluted to 100 µg/mL. Then, the hydrodynamic diameter and zeta potential were measured by DLS using the Zetasizer (3000HS, Malvern Instruments Ltd., UK). The morphological examination was further performed by transmission electron microscope (TEM, JEM1230, JEOL, Japan). Briefly, the samples were placed on a copper mesh, air dried naturally and then subjected to TEM observation.

Drug loading content

The drug loading content of PL/ACC/Sim and Tc/ACC/Sim were analyzed by a high-performance liquid chromatography (HPLC) with an Agilent ZORBAX SB-C18 column (4.6 mm×150 mm, 5 µm). The constant flow rate was 1 mL/min and the column temperature was 35 °C. What is more, the detection ultraviolet wavelength was at 239 nm. The formulated PL/ACC/Sim and Tc/ACC/Sim dispersions were destroyed by adding a mixed solution (1:1 ratio of 0.6 M HCl : ethanol). Then, Sim was separated by centrifugation at 20000 rpm for 15 min. The concentration of free Sim in the supernatant was measured. The drug loading (DL%) of Sim were calculated using the following formula:

$$DL\% = (W_0 - W_a) / (W_0 - W_a + W) \times 100\%$$

W_0 is the total weight of drugs added to the system, W_a represents the weight of free drug in the supernatant, W represents total weight of the system.

MC3T3-E1 cell culture

Clonal newborn mouse calvaria MC3T3-E1 cells were used as model cells to explore the behavior of nanocarrier in normal cells, which were cultured in α MEM medium containing 10% (v/v) FBS. When osteoblast differentiation and mineralization experiments were performed, 10 mmol/L β -glycerophosphate and 50 µg/L L-ascorbic acid were added to the basic medium. In addition, the cell culture medium was changed every other day [28].

In vitro cellular uptake and in vivo bone targeting of Tc/ACC

MC3T3-E1 cells were seeded at 1×10^5 cells/well in 12-well plates and incubated for 24 h until they were attached to the wells. Subsequently, cells were treated with fresh medium containing ODA-FITC labeled PL/ACC and Tc/ACC. To prepare the ODA-FITC labeled PL/ACC and Tc/ACC, ODA-FITC was added to the equivalent lipid component of blank

PL/ACC and Tc/ACC (ODA-FITC: PL =1:10, w/w). Then ODA-FITC labeled PL/ACC and Tc/ACC were prepared as mentioned above. At predetermined intervals (2, 4, 6, 10 h) the cells were collected and observed under a confocal microscope (Olympus, Japan). In addition, semiquantitative analysis of cellular uptake was assessed with the flow cytometry (FC500MCL, Beckman Coulter, USA).

All animal experiments were approved by the Animal Care and Use Committee of Zhejiang University in accordance with the guidelines for the care and use of laboratory animals. The bone-targeting ability of PL/ACC and Tc/ACC was evaluated in ICR mice. The fluorescence dye ICG was used to detect the behavior of PL/ACC and Tc/ACC, which was loaded into the PL during drug loading (same as FITC labeling). Six ICR mice were randomly divided into two groups, three mice per group. ICG labeled PL/ACC and Tc/ACC were injected into mice through the tail vein. After 48 h, the mice were sacrificed, and their main organs (heart, liver, spleen, lungs, and kidneys) and the femur and tibia of the hind leg bones were obtained. The fluorescence intensity of the obtained organs and legs were subsequently detected with a Maestro EX *in vivo* imaging system (Maestro, USA) and calculated as a percentage using the following equation:

$$\text{Distribution of fluorescence intensities (\%)} = \frac{A_{\text{tissue}}}{A_{5\%}} \times 100\%$$

A_{tissue} is the fluorescence intensity of the major organs, and $A_{5\%}$ is the fluorescence intensity of ICG labeled PL/ACC or Tc/ACC at an injected dose of 5%.

In vitro bone targeting of Tc/ACC

To investigate the bone mineral binding ability between bone-like substrates and bone-targeted delivery system *in vitro*, hydroxyapatite (HAP) assay was performed according to the previous report [29, 30]. In brief, the initial fluorescence intensity of ODA-FITC labeled PL/ACC and Tc/ACC was measured (Ex [excitation wavelength] =496 nm, Em [emission wave-length] =523 nm, slit [width of slit] =5 nm, U [voltage of the photomultiplier] =700 V) using a fluorescence spectrometer (F-2500; Hitachi Ltd, Tokyo, Japan). Then, 20 mg HAP was added to the ODA-FITC labeled PL/ACC and Tc/ACC (2 mL aqueous solution, 1 mg/mL). The suspensions were stirred under room temperature with gentle mechanical stirring for 1 hour to allow the adsorption of the ODA-FITC labeled PL/ACC and Tc/ACC onto the HAP. The amount of the ODA-FITC labeled PL/ACC and Tc/ACC adsorbed was determined by measuring the difference between the fluorescence

intensity of the initial stock solution and the supernatant after adsorption, according to the following equation:

$$\text{HAP absorption affinity} = (I_0 - I_a) / I_0$$

where I_0 represents the initial fluorescence intensities of the initial stock solution and I_a represents the fluorescence intensities of the supernatant after 1 hour adsorption.

Optimization of administration dosage

We firstly evaluated the toxicity of the constructed nanocarriers (PL/ACC and Tc/ACC) to cells using MTT method. Afterwards, the Sim loaded DDSs were tested under different given drug concentration to explore the optimal concentration of Tc/ACC/Sim for osteoblast differentiation and mineralization. MC3T3-E1 cells were seeded at 1×10^4 cells/well in 96-well plates and incubated for 24 h, after which cells were exposed to a series of concentrations of PL/ACC, Tc/ACC, Sim, PL/ACC/Sim and Tc/ACC/Sim for 48 h, after which 20 μL of 5 mg/mL MTT was added to each well for another 4 h followed by adding 200 μL of DMSO into each well to dissolve the forming formazan crystals. Subsequently, these plates were stirred at 37 °C for 30 min, and the absorbance of each well at 570 nm was measured by an automatic microplate reader.

In vitro osteoporosis reversing effect

MC3T3-E1 cells were seeded at 1×10^5 cells/well in 12-well plates and cultured in osteogenic differentiation and mineralization medium, which included Tc/ACC, Sim, PL/ACC/Sim and Tc/ACC/Sim (the concentration of Sim was 10^{-7} mol/L and the concentration of Ca^{2+} of Tc/ACC was the same as Tc/ACC/Sim) for 14 days. After 14 days of culture, the cells were fixed with 70% ethanol for 1 h, and subsequently stained using alizarin red S at the concentration of 1.5% at pH 4.0-4.2 for 10-15 min. Unreacted dye was removed and the formed mineralized nodules were observed with a light microscope. Finally, 10% cetylpyridinium chloride was added to each well to dissolve the alizarin red S in the cell matrix, and the concentration of alizarin red S was calculated by measuring the UV absorbance of the sample at 562 nm.

Besides, MC3T3-E1 cells were cultured in osteogenic differentiation and mineralization medium which includes Tc/ACC, Sim, PL/ACC/Sim and Tc/ACC/Sim as mentioned above for 7 days. After 7 days of culture, the MC3T3-E1 cells were lysed with PBS with 0.1% Triton X-100 under ultrasound. Afterwards, ALP activity was measured using an ALP test kit.

Western blotting assay

MC3T3-E1 cells were seeded in plates and cultured in osteogenic differentiation and mineralization medium containing PL/ACC (the concentration of Ca^{2+} was 0.25 $\mu\text{g}/\text{mL}$). After 3 days of culture, MC3T3-E1 were lysed by the addition of cold RIPA lysis buffer and subjected to western blotting assay as reported in our previous study using corresponding antibodies (p-Smad and BMP-2) [31].

In vivo osteoporosis reversing effect

Female Sprague Dawley rats, which had a mean body weight of 180-200 g were housed in a climate-controlled environment with a 12/12 h light/dark cycle with access to standard food and water.

Thirty female Sprague Dawley rats were randomly divided into six groups with five mice in each group: the SHAM group, the OVX group, the TC/ACC group and the Sim group, the PL/ACC/Sim group, the Tc/ACC/Sim group with a Sim dose of 1 mg/kg/2 days. All groups except the SHAM group were all bilaterally ovariectomized, whereas the SHAM group was subjected to a sham operation of abdominal invasion. The experimental groups were subjected to intravenous administration starting 1 month after bilateral ovariectomy, whereas the SHAM and OVX groups were administered saline. After 2 months of administration, all animals were sacrificed. The main organs (heart, liver, spleen, lungs and kidneys) and the femurs of rats were obtained. The excised organ samples (heart, liver, spleen, lungs and kidneys) of every animal were stained with H&E, after which they were observed with a light microscope (Nikon, ECLIPSE Ni).

Micro-CT was employed to analyze some changes in the trabecular bone of the femur. A SkyScan-1176 (Bruker micro CT, Belgium) system (18 μm voxel size, 90 kV, 278 μA , 230 ms exposure time, Al 0.5 mm filter, 180° rotation step) was used for the examinations. The 1.6 version of NR econ software (Bruker micro CT, Belgium) was used for 3D reconstruction and viewing of images. After 3D reconstruction, the 1.13 version of CT software (Bruker micro CT, Belgium) was used for bone analysis. The index included bone mineral density (BMD), bone volume fraction (BV/TV), thickness (Tb. Th), number (Tb. N) and separation (Tb. Sp) were all calculated to evaluate the bone formed in the defect area.

As mentioned earlier, Sim has the potential to increase the activity of BMP-2 and promote the formation of new bone *in vitro* and in animals through the BMP-Smad signaling pathway. During this process, ALP activity increases and tartrate-resistant acid phosphatase (TRAP) activity decreases. To

evaluate the pharmacodynamic effect of Sim, all femurs were decalcified in EDTA, after which the femur were dehydrated and then embedded in paraffin. Then, sections (4 μm thickness) were stained with ALP and TRAP.

Besides, all femurs were decalcified in EDTA, dehydrated, and then embedded in paraffin to obtain sections of 4 μm thickness, which were then stained with hematoxylin and eosin (HE). In addition, the osteogenic effects of Sim and Ca^{2+} were assessed by immunohistochemistry (IHC) analysis of osteopontin (OPN) and osteocalcin (OCN). To further explore the mechanism of bone formation, IHC staining of BMP-2 was also performed.

Results and Discussion

Characterization of Tc/ACC/Sim

The Tc-SA as a key targeting moiety was firstly synthesized using chemical reaction. The carboxyl group from SA and the hydroxyl group from Tc were conjugated using EDC and HBOT as the catalyzers. The finally obtained Tc-SA was characterized using ^1H NMR. As displayed in Figure 1, the peaks at 0.96 ppm and 1 ppm corresponded to the $-\text{CH}_3$ and $-\text{CH}_2$ of SA, respectively. In addition, the peak of $-\text{COOH}$ from SA was also observed at 13 ppm. Accordingly, peaks at 7.0-8.0 ppm were assigned to the hydrogens of the benzene ring of Tc. As expected. The peaks of $-\text{CH}_3$ and $-\text{CH}_2$ from SA as well as peaks of the benzene ring from Tc were all clearly shown in the spectrum of Tc-SA while the peak of $-\text{COOH}$ was disappeared. These results strongly suggested the successful preparation of Tc-SA through esterification reaction between the carboxyl group of SA and the hydroxyl group of Tc. The conjugation degree of Tc on SA was calculated to be 53.48% according to the results of ^1H NMR.

Afterwards, the preparation of Tc/ACC/Sim from ACC was investigated by monitoring the particle size distribution, morphology as well as zeta potential. As shown in Figure 2A, the ACC prepared using vapor-diffusion method was composed of numerous nano-sized particles with Z-average diameter around 110.24 ± 1.88 nm with a surface charge of 31.7 ± 0.23 mV. The surface modification of PL and Tc slightly increased the size of Tc/ACC to around 129.27 ± 1.53 nm (Z-average) with a significantly reversed surface charge to -15.3 ± 0.12 mV. The increase in size and the reverse in surface charge strongly indicated the successful anchoring of PL and Tc-SA on the surface of ACC, which was beneficial for the preserving of the water responsive nature of ACC and the targeting to osteoporosis tissues. After loading of Sim, the size of the obtained

Tc/ACC/Sim further increased to 166.58 ± 4.76 nm (Z-average) with a constant surface charge of -13.2 ± 0.18 mV, which suggested that the Sim was loaded into the PL layer of Tc/ACC instead of being adsorbed on the surface of the nanoparticles. The Tc-SA unmodified PL/ACC/Sim was also constructed to investigate the effect of modification on the change in size and surface charge. The results (Figure 2A) revealed that the particle size of PL/ACC/Sim (182.00 ± 6.06 nm, Z-average) was similar to that of Tc/ACC/Sim with a comparable surface charge of -12.6 ± 0.15 mV, indicating that Tc-SA modification showed minor influence on the nanoparticle formation. The morphology observation using TEM was in Figure 2B. The results revealed that ACC was spheroid nanoparticle with independent boundary to one another. The following modification of PL and Tc-SA, as well as drug loading, showed insignificant influence on the morphology of the nanoparticles. As a result, the finally obtained Tc/ACC/Sim was well dispersed spheroid nanoparticle at the size range of around 100 nm, which was beneficial to maintain stable in the circulation for better osteoporosis therapy.

The linear relationship of the HPLC method adopted in our study for Sim determination was $y=287.47x-53.604$ ($R^2=1$) with lowest detectable limit of 1.0 $\mu\text{g}/\text{mL}$. The DL of PL/ACC/Sim and Tc/ACC/Sim was $8.80 \pm 0.30\%$ and $7.90 \pm 0.38\%$, respectively, which were sufficient for the osteoporosis therapy.

In vitro cellular uptake and bone targeting of Tc/ACC

ODA-FITC was synthesized and inserted into the PL layer of Tc/ACC as the probe to indicate the location of the DDS. MC3T3-E1 cells were treated by Tc/ACC or PL/ACC with or without Tc modification to explore the cellular uptake profile of the nanoparticles. As shown in Figure 3A, green fluorescence signal can be readily observed within MC3T3-E1 cells at merely 2 h post incubation and extended incubation resulted in further increased fluorescence signal in cells, which suggested the preferable internalization of both nanoparticles in MC3T3-E1 cells. Moreover, it was observed that although there were some variations in cellular uptake during the tests, compared to that of PL/ACC group, the Tc modification did not significantly change the uptake of Tc/ACC into MC3T3-E1 cells as time extended, which was also supported by the semiquantitative analysis using flow cytometry (Figure 3B). Further cellular uptake investigation using drug loaded nanoparticles revealed similar results (Figure S1). All results suggested that instead

of specifically targeting the HAP in bone tissue, the Tc modification exerted minor influence on the endocytosis of nanoparticles into MC3T3-E1 cells which might be beneficial for the Sim delivery in the targeted cells after accumulation in the bone tissue. Moreover, the Tc/ACC with similar size and surface charge to that of PL/ACC might be suitable to serve as the carrier in the following studies.

The *in vitro* bone targeting of Tc/ACC was firstly investigated using HAP absorption assay. The HAP

was employed to simulate the exposed bone tissues in osteoporosis site. As shown in Figure 4A, after 1 h of incubation, significant difference in fluorescence intensity was found between the supernatant of PL/ACC and Tc/ACC groups. In detail, almost 75% of the Tc/ACC was absorbed by the HAP while the percentage drastically dropped to merely 4.7% in PL/ACC group, which strongly suggested the preferable binding of Tc to HAP for enhanced bone targeting.

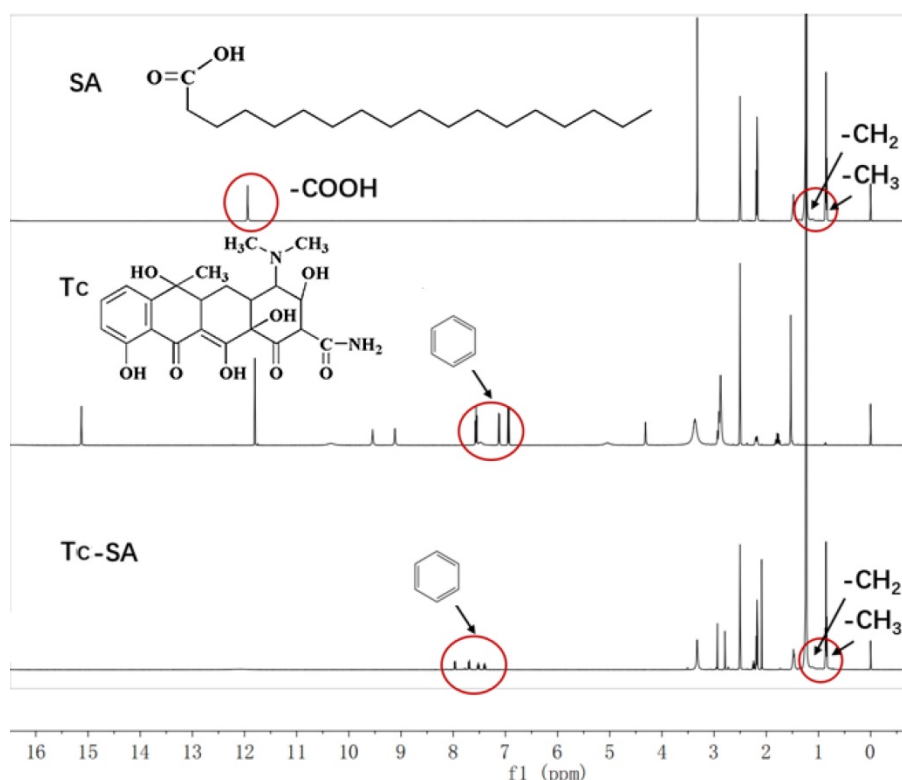


Figure 1. Characterization of Tc-SA using ^1H NMR. Inserted images were corresponding chemical structure and peak assignments.

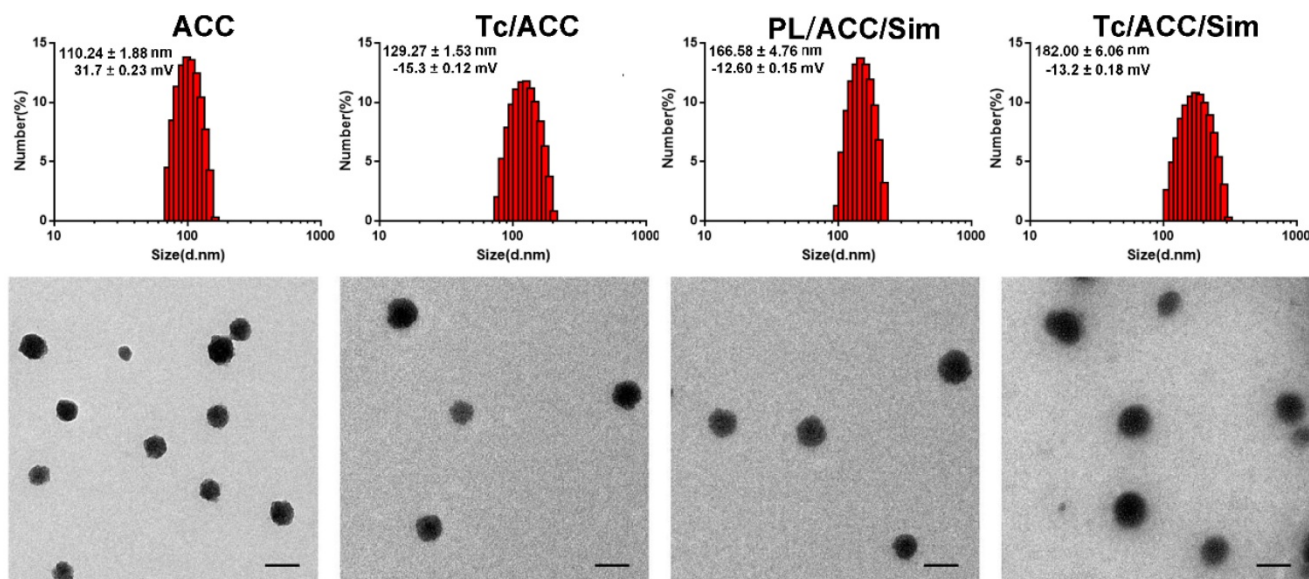


Figure 2. Characterization of Tc/ACC from ACC using (A) dynamic light scattering (DLS) and (B) transmission electron microscopy (TEM) images. Scale bar: 100 nm.

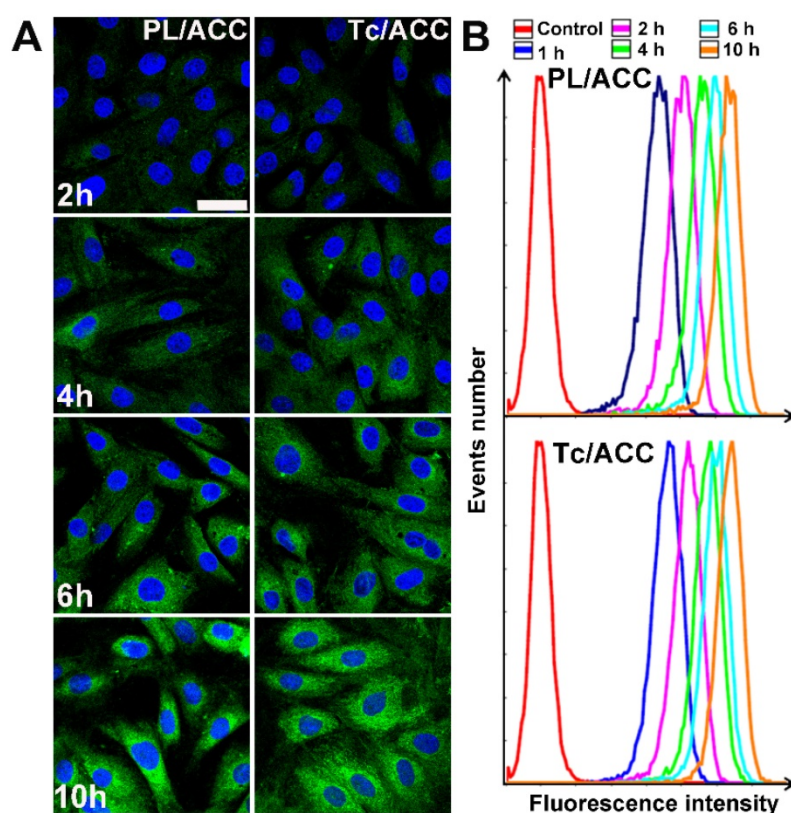


Figure 3. *In vitro* cellular uptake of Tc/ACC. MC3T3-E1 cells were incubated with ODA-FITC labeled PL/ACC and Tc/ACC for different time intervals (2, 4, 6, 10 h) and then subjected to observation using confocal microscope. **(A)** Time-dependent cellular uptake of ODA-FITC labeled PL/ACC and Tc/ACC. Scale bar: 30 μ m. **(B)** Semi-quantitative analysis of cellular uptake by flow cytometry.

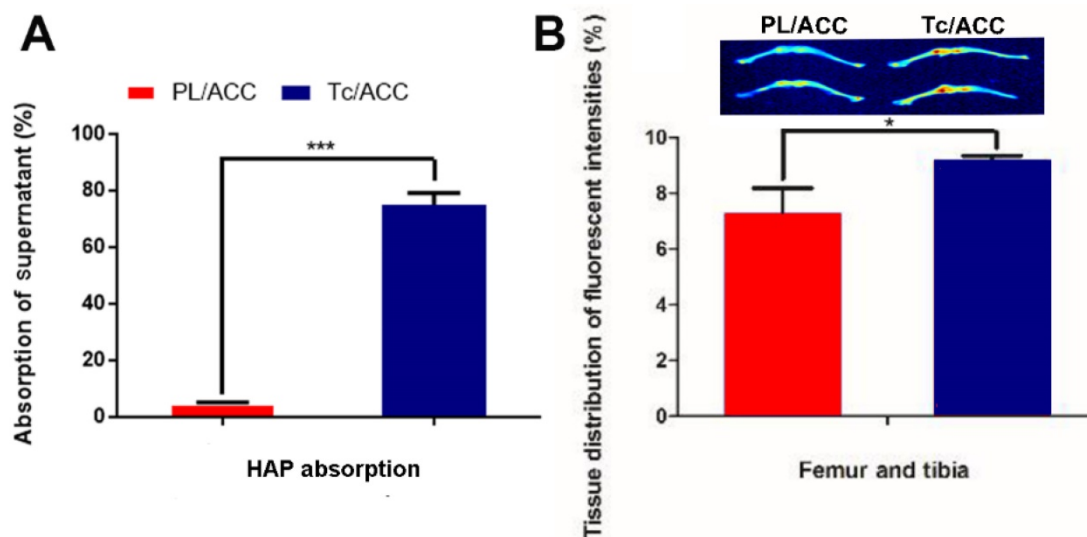


Figure 4. Bone targeting of Tc/ACC. **(A)** *In vitro* bone targeting of Tc/ACC using HAP adsorption assay. HAP was added to the ODA-FITC labeled PL/ACC and Tc/ACC and incubated for under gentle mechanical stirring for 1 hour. Afterwards, the decrease in the fluorescence of the supernatant was measured. **(B)** *In vivo* bone targeting of Tc/ACC using fluorescence imaging. ICR mice were randomly divided into two groups and intravenously injected with ICG labeled PL/ACC and Tc/ACC. At 48 h post administration, the mice were sacrificed and the quantitative accumulation of fluorescence signal in the femur, and tibia bones were calculated. Inset image was fluorescence images of the distribution of ICG labeled PL/ACC and Tc/ACC in the femur and tibia bones. Results were expressed as mean \pm S.D. ($n = 3$).

Afterwards, the *in vivo* bone targeting of Tc/ACC in normal ICR mice was also investigated using ICG as the probe. It was noted that the fluorescence intensities in the bone of the Tc/ACC group were obviously higher than those in the PL/ACC group (inserted image in Figure 4B). These results suggested

that the Tc modification was beneficial for the targeted accumulation of Tc/ACC to the bone tissue, which was favorable in osteoporosis therapy.

In order to further confirm this conclusion, the fluorescence intensities in bone tissues were quantified by corresponding software. As shown in

Figure 4B, 25.72% more Tc/ACC was detected in the femur and tibia than the PL/ACC group. Both the *in vitro* and *in vivo* results confirmed that Tc/ACC could target bone tissue and accumulate at bone sites, which suggested the potential of Tc/ACC for bone-targeted delivery.

Optimization of administration dosage

In order to find the optimized administration dosage, the cytotoxicity of drug free carriers and DDSs on MC3T3-E1 cells were investigated individually. As shown in Figure 5A, both Sim free PL/ACC and Tc/ACC showed low cytotoxicity on cells with 50% cellular growth inhibition (IC_{50}) value of $4428.3 \pm 208.8 \mu\text{g/mL}$ and $3754.3 \pm 88.3 \mu\text{g/mL}$ ($n=3$), respectively. The reduce in IC_{50} in Tc/ACC might related to the antibiosis nature of Tc, which demonstrated that the hybrid nanocarriers using naturally originated PL and ACC exerted high biocompatibility on cells and were suitable for the safe delivery of drugs. Afterwards, the Sim loaded DDSs were tested under different given drug concentrations to explore the optimal concentration of Tc/ACC/Sim for osteoblast differentiation and mineralization. As shown in Figure 5B, all Sim containing groups showed a concentration dependent toxic effect on MC3T3-E1 cells. However, it was noted that Sim loading using the hybrid carrier composed of PL and ACC significantly reduced the cytotoxicity induced by Sim, especially when the concentration of Sim was higher than 1×10^{-6} mol/L, which was in line with previous reports that DDS can effectively reduce the side effects of loaded drugs [27, 32]. Considering the cytotoxicity effect of Tc on MC3T3-E1 cells, the comparative cytotoxicity between PL/ACC/Sim and Tc/ACC/Sim was investigated. It was demonstrated that no significant cytotoxicity difference was observed between PL/ACC/Sim and Tc/ACC/Sim on MC3T3-E1 cells, suggesting that the modification of Tc under the tested concentrations exerted almost negligible cytotoxicity effect. Moreover, it was observed that when the concentration of Sim was higher than 1×10^{-7} mol/L, the cytotoxicity of cells in Sim group fell below 90%. As a result, in order to exclude cytotoxicity effects of Sim on the differentiation and mineralization of cells, the drug concentration at 1×10^{-7} mol/L was selected in the following experiments unless otherwise stated.

In vitro osteoporosis reversing effect

In order to evaluate the osteoporosis reversing effect of Tc/ACC/Sim, its influence on osteoblast mineralization was firstly assessed by quantitative mineralization experiments. MC3T3-E1 cells were

cultured in standard osteogenic differentiation and mineralization medium containing 10 mM β -glycerophosphate, 50 $\mu\text{g/mL}$ ascorbic acid and different formulations at the equal Sim concentration of 1×10^{-7} mol/L for 14 days [33]. As shown in Figure 6A, the increased mineralized nodules (indicated by arrows) can be observed in the group cultured with free Sim when compared to the control group, which might due to the potential of Sim to increase BMP-2 expression in osteoblasts and promote the differentiation and mineralization of osteoblasts through the BMP-Smad signaling pathway. On the other hand, it was noted that calcium supplement using Tc/ACC carrier also showed beneficial effects on osteoblasts than untreated group, which suggested the positive effect of calcium supplement in reversing osteoporosis. Further investigation using western blotting further confirmed that BMP-Smad signaling pathway was involved in this benefit (Figure S2) as a result of calcium supplement. In particular, the combination of calcium supplement and osteoblasts promotion using ACC and Sim (PL/ACC/Sim and Tc/ACC/Sim) showed further enhanced benefits on osteoblast mineralization. The quantitative analysis of alizarin red S staining was also performed and displayed in shown in Figure 6B. In line with results obtained in Figure 6A, the quantitative analysis also revealed that mono therapy using either calcium supplement or osteoblasts promotion could exert beneficial effects on osteoblast mineralization while the combination of both approaches could further elevated the final outcome, suggesting the promising synergetic effects of this strategy.

Sim has the potential to increase BMP-2 expression and promote the formation of new bone *in vitro*. ALP is an up-regulated enzyme with positive relation to the osteoblast differentiation, which was considered as a marker of new bone formation [34]. As a result, we examined the expression of ALP in MC3T3-E1 cells treated with different formulations. As shown in Figure 6C, compared with control group, the Tc/ACC group showed certain elevation on the ALP activity, which further confirmed the positive effect of calcium supplement in osteoblast differentiation for osteoporosis therapy. Additionally, in line with previous reports, it was noted that all Sim containing groups could significantly increase the ALP activity in MC3T3-E1 cells [35, 36]. In particular, the Sim-loaded DDSs showed comparable benefits to that of free Sim, which suggested that the loaded Sim was able to be effectively released from the DDSs to realize osteoblast promotion.

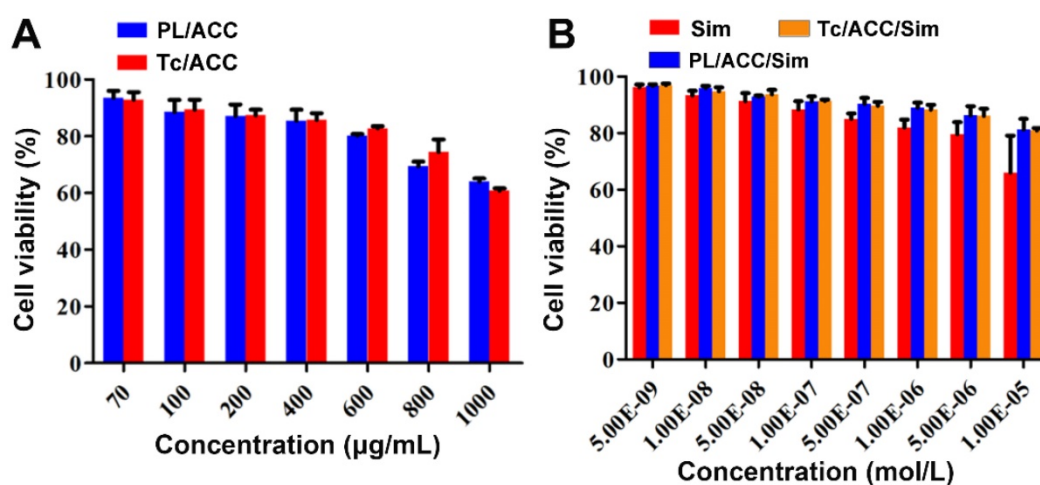


Figure 5. Optimization of administration dosage. MC3T3-E1 cells were exposed to a series of concentrations of PL/ACC, Tc/ACC, Sim, PL/ACC/Sim and Tc/ACC/Sim for 48 h. Afterwards, the cell viability influence of (A) Sim free carrier (PL/ACC and Tc/ACC) and (B) Sim containing formulations were evaluated using MTT assay. Results were expressed as mean \pm S.D. ($n = 3$).

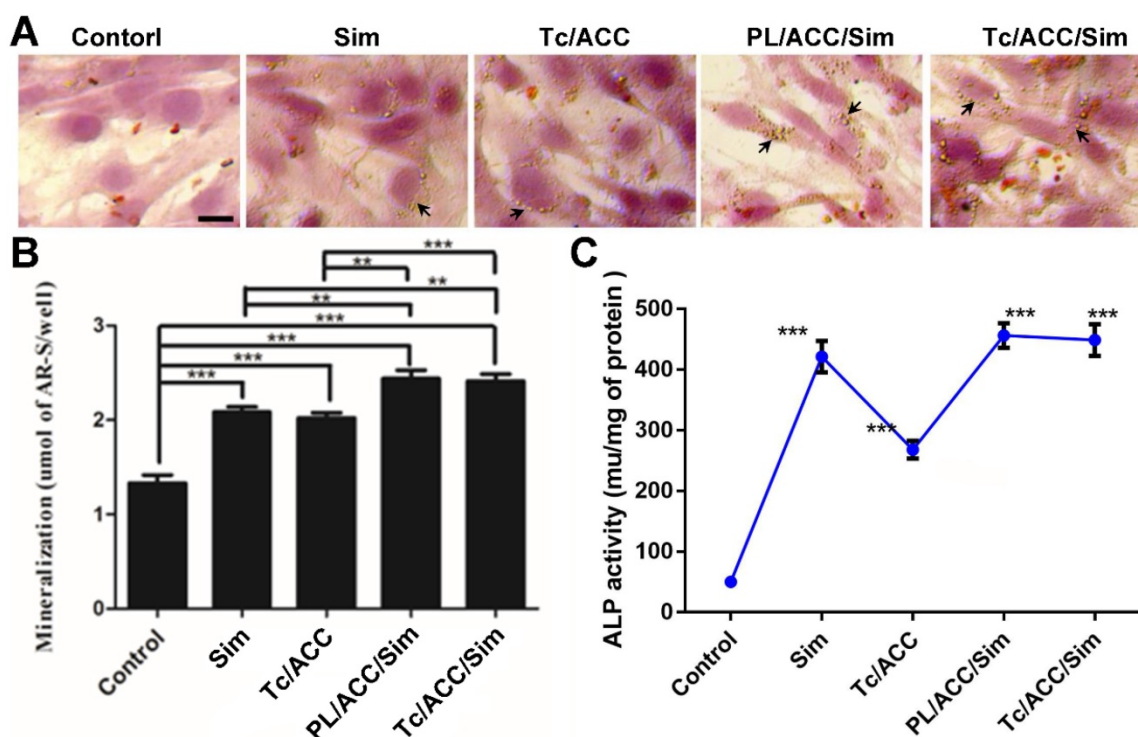


Figure 6. Effects of Sim-loaded nanoparticles on mineralized nodule formation and ALP activity in MC3T3-E1 cells. MC3T3-E1 cells were cultured in standard osteogenic differentiation and mineralization medium containing 10 mM β -glycerophosphate, 50 μ g/mL ascorbic acid and different formulations at the equal Sim concentration of 10^{-7} M). Afterwards, the mineralization of the extracellular matrix was evaluated by optical microscopy and macroscopic observation (A), quantitative mineralization results (B) at 14 days post incubation, and stimulation of ALP activity (C) at 7 days post incubation. Results were expressed as mean \pm S.D. ($n = 3$). * $p < 0.05$, ** $p < 0.01$, *** $p < 0.001$, significant differences compared with the control.

In vivo osteoporosis reversing effect

Micro-CT scanning was used to analyze the trabecular bone mineral density (BMD, Figure 7A), trabecular bone volume percentage (BV/TV, Figure 7B), trabecular separation (Tb. Sp, Figure 7C), trabecular thickness (Tb. Th, Figure 7D) and trabecular number (Tb. N, Figure 7E) at 12 weeks post-treatment. In Figure 7A, the femur BMD was distinctly different between the SHAM group and the OVX group, with a value of 0.186 ± 0.007 g/cm² in the

SHAM group and 0.118 ± 0.002 g/cm² in the OVX group. The BMD of the OVX group was reduced by 36.56% compared to that in the SHAM group, indicating that the osteoporotic model rats were established successfully [37].

BMD and BV/TV are extensively used as predictors for evaluating osteoporosis [38]. In our study, OVX treatment significantly decreased the BMD and BV/TV in rats, while mono therapy using either calcium supplement or osteoblasts promotion

could significantly reverse this process. Previous reports have revealed that Sim can increase BMP-2 expression in osteoblasts and promote the formation of new bone through the BMP-Smad signaling pathway [39, 40], which was confirmed by the increased BMD and BV/TV in all Sim treated groups in our study. In particular, combination therapy (PL/ACC/Sim and Tc/ACC/Sim) further enhanced the effect with a better performance. Similar tendencies were also observed in Tb. Th and Tb. N groups when compared to the OVX group. Accordingly, OVX increased the Tb. Sp of treated subjects at the end of the test while the combination of calcium supplement and osteoblasts promotion could significantly reverse this process than applying mono therapy alone. These results indicated that Sim could stimulate bone formation by promoting osteoblast differentiation and mineralization, thereby repairing damaged bone tissue and the synergetic effects using calcium supplement could exert further beneficial effects on the therapy. Moreover, it was noted that Tc/ACC/Sim showed better performance than PL/ACC/Sim in all experiments, which provided decisive evidence to prove the promising bone targeting of Tc/ACC/Sim and its positive effects in osteoporosis therapy.

The 2D images and 3D images of trabecular bone were also measured by micro-CT to confirm the above

mentioned conclusion. As shown in Figure 8, OVX resulted in significant trabecular bone loss in the subjects, which resulted in osteoporosis. In line with above results, both calcium supplement and osteoblast promotion significantly alleviated the osteoporosis and increased the compact bone substance as compared to OVX group, indicating a significant improvement in microstructure and bone volume. As expected, the synergetic effects of calcium supplement/osteoblast promotion and Tc modification (Tc/ACC/Sim group) further increased the health of trabecular bone which achieved the best microstructure and bone volume in the micro-CT assay.

During the process of BMP-2-induced osteoblast differentiation, Runx2 expression and ALP activity increase as the result of BMP-Smad signaling pathway activation [41]. As shown in Figure 9A, in either ACC or Sim containing groups, the activity of ALP was higher than that of the OVX group. In detail, several cells were brought together, and the surrounding gray area suggested the newly formed bone matrix where the activity of ALP was high, indicating that new bone was forming. These results were also confirmed by the mean optical density (MOD) studies in Figure S3. As a result, it was inferred that the beneficial effects of calcium supplement in reversing osteoporosis were

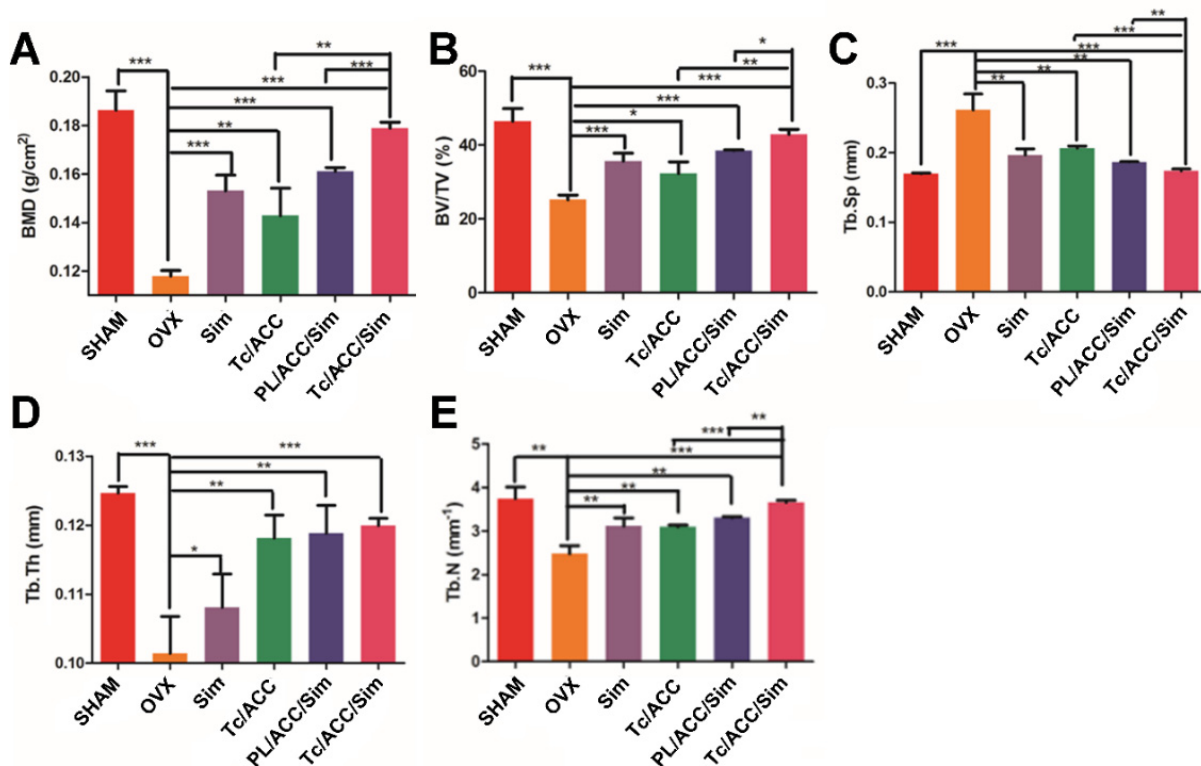


Figure 7. Female Sprague Dawley rats were randomly selected and subjected to sham operation or bilaterally oophorectomy. The treatment groups were intravenously administered with Sim, PL/ACC/Sim or Tc/ACC/Sim group at the Sim dose of 1 mg/kg/2 days for 2 months. Afterwards, the rats were sacrificed and the micro-CT analysis of bone tissue from each group was conducted. (A) Trabecular bone density (BMD); (B) Trabecular bone volume percentage (BV/TV); (C) Trabecular separation (Tb.Sp); (D) Trabecular thickness (Tb.Th) and (E) trabecular number (Tb.N) of the femur. Results were expressed as mean \pm S.D. ($n = 3$). * $p < 0.05$, ** $p < 0.01$, *** $p < 0.001$, significant differences compared with the control.

also partially attributed to the BMP-2-induced osteoblast differentiation [42], which finally resulted in synergistic osteoblast promotion with Sim for better osteoporosis therapy. As expected, the calcium supplement (using ACC) or osteoblast promotion (using Sim) significantly reduced the TRAP activity than that in OVX group. Most importantly, in line with above assays, in both experiments, the combination of calcium supplement and osteoblast promotion achieved the better performance than mono therapy. In addition, the modification of Tc could increase the distribution of Tc/ACC/Sim in the bone and increase the concentration of Sim at the bone site. Therefore, the ALP activity of the Tc/ACC/Sim groups was the highest and almost the same as that of the SHAM group. Accordingly, the TRAP activity of Tc/ACC/Sim was as low as that of the SHAM group [43].

In order to further confirm the above conclusions, all sections of femurs were evaluated histologically (Figure 9B and Figure S4). As displayed in Figure 9B, normal compactness of the femur and competent trabeculae were observed in the SHAM group, while the OVX group showed sparse loss of interconnectivity and thinning of the trabeculae, thereby showing widened intertrabecular spaces. The OVX group showed more adipose tissue than the other groups did. There was a statistically significant increase in trabecular interconnectivity in the all Sim containing groups in comparison to the OVX group. Moreover, the trabecular bone was much more prominent in the Tc/ACC/Sim group than that in PL/ACC/Sim due to the bone-targeting ability of Tc, thus increasing the accumulation of Sim in bones and

increasing the drug efficacy. It is also noted that the Tc/ACC/Sim treated group showed more resemblance to the SHAM group. Overall, the bone histological analysis indicated a remarkable recovery effect of Sim and showed a restored architecture with this treatment regime in the ovariectomy-induced osteoporosis model in rats [44].

In order to confirm that BMP-Smad signaling pathway was involved in the osteoporosis reversing process of calcium supplement and to further determine the synergistic benefits of calcium supplement on the osteoblast promotion with Sim, the IHC staining of different groups was performed and shown in Figure 9C and Figure S5. Sim could promote the differentiation and mineralization of osteoblasts through the BMP-Smad signaling pathway, therefore, we can study the efficacy of Sim by studying the expression of BMP-2 protein and the mineralization markers OPN and OCN. As shown in Figure 9C, compared to that in OVX group, all three markers were significantly evaluated in Tc/ACC group. As expected, these three markers were also highly expressed in all Sim containing groups. In particular, the Tc/ACC/Sim group integrated Tc targeting and synergetic therapy showed the most satisfying performance (expression of BMP-2, OPN and OCN) among all formulations which was comparable to that of SHAM group. These results indicated that calcium supplement in combination with Sim could preferably induce synergistic osteoblastic differentiation through the BMP-Smad signaling pathway and the DDS using Tc as the targeting moiety could specifically transport more drugs to the bone for better osteoporosis therapy [45].

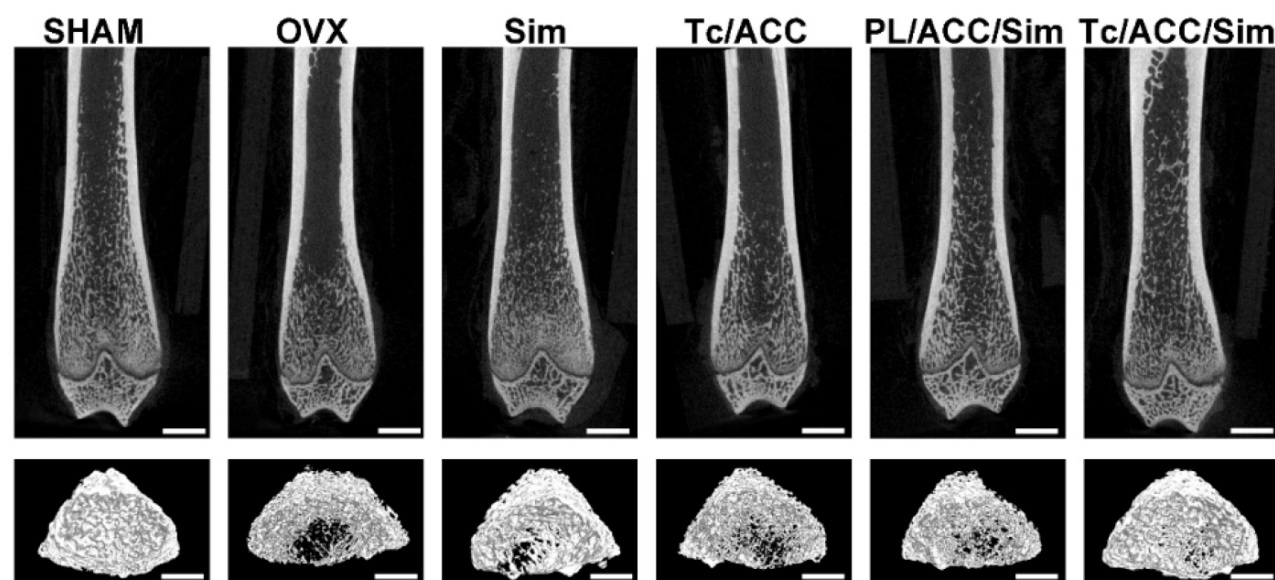


Figure 8. The 2D and 3D images of trabecular bone measured by micro-CT. Scale bar: 1mm.

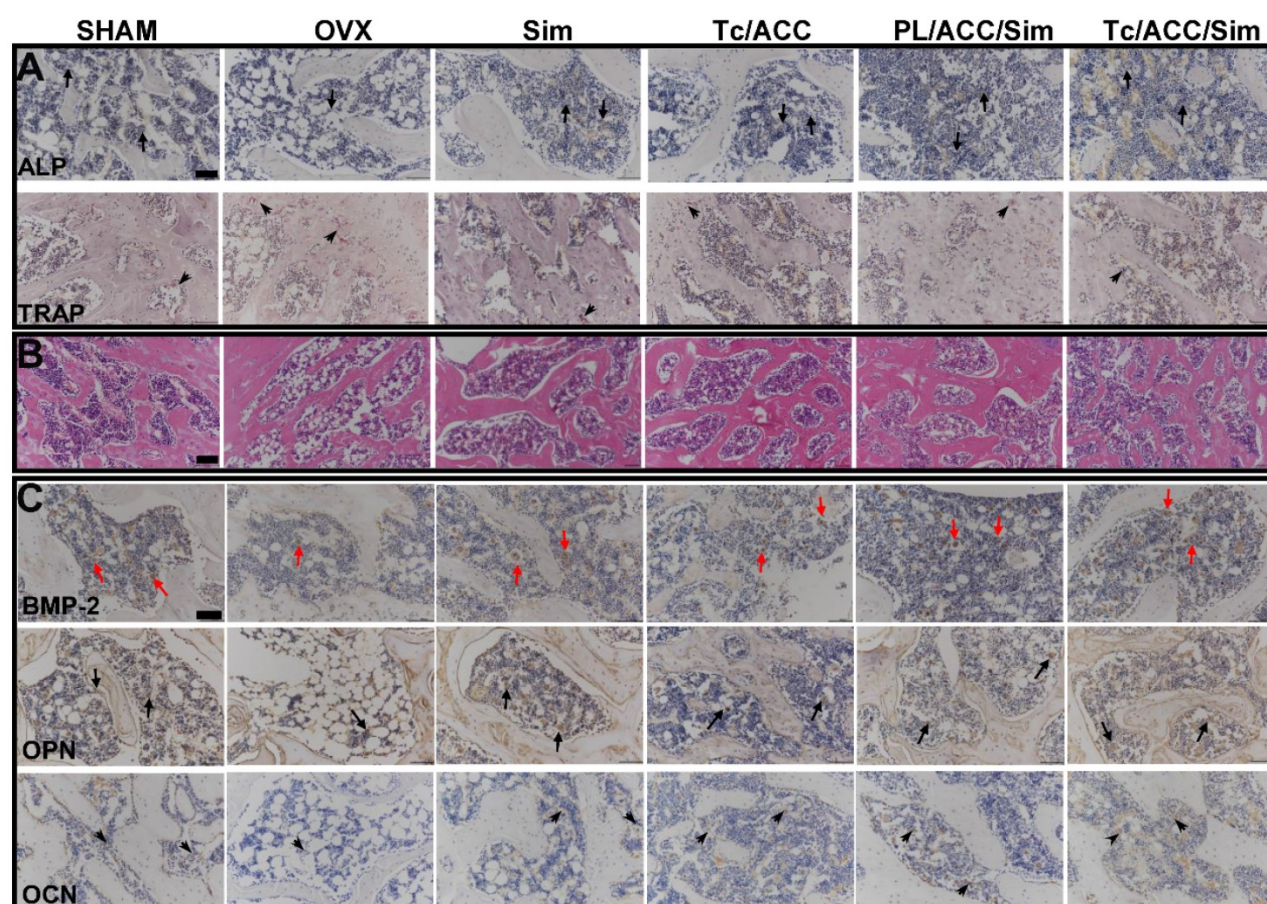


Figure 9. (A) ALP activity (arrows) and TRAP assay results (arrowheads) of bone tissue sections. (B) Histological assessment of bone formation in each group using HE staining. (C) Immunohistochemical staining for BMP-2 in typical newly-formed bone tissue (red arrows) and immunohistochemical staining for the osteogenic markers OPN (arrows) and OCN (arrowheads). Scale bars = 100 μ m.

Conclusion

In this study, we developed a novel Tc modified ACC carrier (Tc/ACC) for the delivery of Sim (Tc/ACC/Sim). The obtained DDS was composed of nanosized particles which showed high biocompatibility on MC3T3-E1 cells. Moreover, Tc modification could enhance the accumulation of the DDS to bones both *in vitro* and *in vivo*. In addition, *in vitro* and *in vivo* osteoporosis reversing assays demonstrated beneficial effects of mono therapy using either calcium supplement or Sim induced osteoblast promotion. Most importantly, the combination of both approaches showed synergistic effects with much more elevated osteoblastic differentiation through the BMP-Smad signaling pathway. Moreover, the Tc modification also potentiated this effect *in vivo* though its bone targeting nature. In summary, the Tc/ACC/Sim integrated Tc targeting and synergetic therapy showed the most satisfying performance both *in vitro* and *in vivo*, which might offer a novel approach for the effective reversing of osteoporosis.

Abbreviations

ACC: Amorphous calcium carbonate
 Tc: Tetracycline
 HAP: Hydroxyapatite
 BMPs: Bone morphogenetic proteins
 TFG: Transforming growth factor
 MMSC: Marrow mesenchymal stem cells
 Sim: Simvastatin
 DDS: Drug delivery system
 PL: Phospholipid
 SA: Stearic acid
 DAPI: 4',6-Diamidino-2-phenylindole
 FITC: Fluorescein isothiocyanate
 DSC: N,N'-disuccinimidyl carbonate
 ODA: Octadecylamine
 EDC: 1-(3-dimethylaminopropyl)-3-ethylcarbodiimide
 HOBT: 1-Hydroxybenzotriazole
 MTT: 3-(4,5-dimethylthiazol-2-yl)-2,5-diphenyl-tetrazolium bromide
 BCA: Bicinchoninic acid
 ALP: Alkaline phosphatase
 ICG: Indocyanine green

αMEM: Alpha-minimum essential medium

¹H NMR: Hydrogen Nuclear magnetic resonance

DLS: Dynamic light scattering

TEM: Transmission electron microscope

HPLC: High-performance liquid chromatography

DL: Drug loading

FBS: Fetal bovine serum

OVX: Ovariectomized

BMD: Bone mineral density

BV/TV: Bone volume fraction

Tb. Th: Bone thickness

Tb. N: Bone number

Tb. Sp: Bone separation

TRAP: Tartrate-resistant acid phosphatase

HE: Hematoxylin and eosin

ICH: Immunohistochemistry

OPN: Osteopontin

OCN: Osteocalcin

Supplementary Material

Supplementary figures.

<http://www.thno.org/v10p8591s1.pdf>

Acknowledgements

This work was supported by the National Natural Science Foundation of China (No. 81773644) and Natural Science Foundation of Zhejiang Province (No. LY18H060002, LY16H180003).

Author Contributions

Jianwei Wang and Shan Tao contributed equally to this work.

All authors have given approval to the final version of the manuscript.

Competing Interests

The authors have declared that no competing interest exists.

References

- Burge R, Dawson-Hughes B, Solomon DH, Wong JB, King A, Tosteson A. Incidence and economic burden of osteoporosis-related fractures in the United States, 2005-2025. *J Bone Miner Res.* 2007; 22: 465-75.
- Duan X, Yang S, Zhang L, Yang T. V-ATPases and osteoclasts: ambiguous future of V-ATPases inhibitors in osteoporosis. *Theranostics.* 2018; 8: 5379.
- Neer RM, Arnard CD, Zanchetta JR, Prince R, Gaich G.A, Reginster JY. et al. Effect of parathyroid hormone (1-34) on fractures and bone mineral density in postmenopausal women with osteoporosis. *N Engl J Med.* 2001; 344: 1434-41.
- Klibanski A, Adams-Campbell L, Bassford TL, Blair SN, Boden SD, Dickersin K. et al. Osteoporosis prevention, diagnosis, and therapy. *J Am Med Assoc.* 2001; 285: 785-95.
- Rachner TD, Khosla S, Hofbauer LC. Osteoporosis: now and the future. *The Lancet.* 2011; 377: 1276-87.
- Raisz LG. Pathogenesis of osteoporosis: concepts, conflicts, and prospects. *J Clin Invest.* 2005; 115: 3318-25.
- Cai M, Yang L, Zhang S, Liu J, Sun Y, Wang X. A bone-resorption surface-targeting nanoparticle to deliver anti-miR214 for osteoporosis therapy. *Int J Nanomed.* 2017; 12: 7469-82.
- Narayanan D, Anitha A, Jayakumar R, Chennazhi KP. In vitro and in vivo evaluation of osteoporosis therapeutic peptide PTH 1-34 loaded PEGylated chitosan nanoparticles. *Mol Pharm.* 2013; 10: 4159-67.

- Sahana H, Khajuria DK, Razdan R, Mahapatra DR, Bhat MR, Suresh S. et al. Improvement in bone properties by using risedronate adsorbed hydroxyapatite novel nanoparticle based formulation in a rat model of osteoporosis. *J Biomed Nanotechnol.* 2013; 9: 193-201.
- Wang C, Chen S, Wang Y, Liu X, Hu F, Sun J. et al. Lipase-Triggered Water-Responsive "Pandora's Box" for Cancer Therapy: Toward Induced Neighboring Effect and Enhanced Drug Penetration. *Adv Mater.* 2018; 30: 1706407.
- Wang C, Han M, Liu X, Chen S, Hu F, Sun J. et al. Mitoxantrone-preloaded water-responsive phospholipid-amorphous calcium carbonate hybrid nanoparticles for targeted and effective cancer therapy. *Int J Nanomed.* 2019; 14: 1503-17.
- Krzeszinski JY, Wei W, Huynh H, Jin Z, Wang X, Chang TC. et al. Lopez-Berestein, miR-34a blocks osteoporosis and bone metastasis by inhibiting osteoclastogenesis and Tgif2. *Nature.* 2014; 512: 431-5.
- Liu W, Wang T, Yang C, Darvell BW, Wu J, Lin K. et al. Alkaline biodegradable implants for osteoporotic bone defects-importance of microenvironment pH. *Osteoporos Int.* 2016; 27: 93-104.
- Wang H, Liu J, Tao S, Chai G, Wang J, Hu FQ. et al. Tetracycline-grafted PLGA nanoparticles as bone-targeting drug delivery system. *Int J Nanomed.* 2015; 10: 5671-85.
- Perrin DD. Binding of tetracyclines to bone. *Nature.* 1965; 208: 787-8.
- Low SA, Kopeček J. Targeting polymer therapeutics to bone. *Adv Drug Deliv Rev.* 2012; 64: 1189-204.
- Li CJ, Liu XZ, Zhang L, Chen LB, Shi X, Wu SJ. et al. Advances in bone-targeted drug delivery systems for neoadjuvant chemotherapy for osteosarcoma. *Orthop Surg.* 2016; 8: 105-10.
- Wang D, Miller SC, Kopečková P, Kopeček J. Bone-targeting macromolecular therapeutics. *Adv Drug Deliv Rev.* 2005; 57: 1049-76.
- Kwak YD, Hendrix BJ, Sugaya K. Secreted type of amyloid precursor protein induces glial differentiation by stimulating the BMP/Smad signaling pathway. *Biochem Biophys Res Commun.* 2014; 447: 394-9.
- Lieberman JR, Daluiski A, Einhorn TA. The role of growth factors in the repair of bone: biology and clinical applications. *JBJS.* 2002; 84: 1032-44.
- Liu DD, Ge K, Jin Y, Sun J, Wang SX, Yang MS, Zhang JC. Teribium promotes adhesion and osteogenic differentiation of mesenchymal stem cells via activation of the Smad-dependent TGF-β/BMP signaling pathway. *J Biol Inorg Chem.* 2014; 19: 879-91.
- Zumbrennen-Bullough KB, Wu Q, Core AB, Canali S, Chen W, Theurl I. et al. MicroRNA-130a is up-regulated in mouse liver by iron deficiency and targets the bone morphogenetic protein (BMP) receptor ALK2 to attenuate BMP signaling and hepcidin transcription. *J Biol Chem.* 2014; 289: 23796-808.
- Mundy G, Garrett R, Harris S, Chan J, Chen D, Rossini G. et al. Stimulation of bone formation in vitro and in rodents by statins. *Science.* 1999; 286: 1946-49.
- Yamashita M, Otsuka F, Mukai T, Otani H, Inagaki K, Miyoshi T. et al. Simvastatin antagonizes tumor necrosis factor-α inhibition of bone morphogenetic proteins-2-induced osteoblast differentiation by regulating Smad signaling and Ras/Rho-mitogen-activated protein kinase pathway. *J Endocrinol.* 2008; 196: 601-13.
- Teitelbaum SC. Stem cells and osteoporosis therapy. *Cell Stem Cell.* 2010; 7: 553-4.
- Yuan H, Chen J, Du YZ, Hu FQ, Zeng S, Zhao HL. Studies on oral absorption of stearic acid SLN by a novel fluorometric method. *Colloids Surf B Biointerfaces.* 2007; 58: 157-64.
- Zhao Y, Luo Z, Li M, Qu Q, Ma X, Yu SH. et al. A preloaded amorphous calcium carbonate/doxorubicin@ silica nanoreactor for pH-responsive delivery of an anticancer drug. *Angew Chem Int Ed.* 2015; 54: 919-22.
- Yang F, Zhao SF, Zhang F, He FM, Yang GI. Simvastatin-loaded porous implant surfaces stimulate preosteoblasts differentiation: an in vitro study. *Oral Surg Oral Med Oral Pathol Oral Radiol Endod.* 2011; 111: 551-6.
- Fu YC, Fu TF, Wang HJ, Lin CW, Lee GH, Wu SC. et al. Aspartic acid-based modified PLGA-PEG nanoparticles for bone targeting: in vitro and in vivo evaluation. *Acta Biomater.* 2014; 10: 4583-96.
- Ho ML, Fu YC, Wang GJ, Chen HT, Chang JK, Tsai TH. et al. Controlled release carrier of BSA made by W/O/W emulsion method containing PLGA and hydroxyapatite. *J Control Release.* 2008; 128: 142-8.
- Wang C, Yu F, Liu X, Chen S, Wu R, Zhao R. et al. Cancer-Specific Therapy by Artificial Modulation of Intracellular Calcium Concentration. *Adv Health Mater.* 2019; 8: 1900501.
- Wang C, Liu X, Chen S, Hu F, Sun J, Yuan H. Facile preparation of phospholipid-amorphous calcium carbonate hybrid nanoparticles: toward controllable burst drug release and enhanced tumor penetration. *Chem Commun.* 2018; 54: 13080-3.
- Gregory CA, Gunn WG, Peister A, Prockop DJ. An Alizarin red-based assay of mineralization by adherent cells in culture: comparison with cetylpyridinium chloride extraction. *Anal Biochem.* 2004; 329: 77-84.
- Wergedal JE, Baylink DJ. Fluoride directly stimulates proliferation and alkaline phosphatase activity of bone-forming cells. *Science.* 1983; 222: 330-2.
- Maeda T, Matsunuma A, Kawane T, Horiuchi N. Simvastatin promotes osteoblast differentiation and mineralization in MC3T3-E1 cells. *Biochem Biophys Res Commun.* 2001; 280: 874-7.
- Park JB, Zhang H, Lin CY, Chung CP, Byun Y, Park YS. et al. Simvastatin maintains osteoblastic viability while promoting differentiation by partially regulating the expressions of estrogen receptors α. *J Surg Res.* 2012; 174: 278-83.

37. Tang Q, Hu Z, Jin H, Zheng G, Yu X, Wu G. et al. Microporous polysaccharide multilayer coated BCP composite scaffolds with immobilised calcitriol promote osteoporotic bone regeneration both in vitro and in vivo. *Theranostics*. 2019; 9: 1125.
38. Legrand E, Chappard D, Pascaretti C, Duquenne M, Krebs S, Rohmer V. et al. Trabecular bone microarchitecture, bone mineral density, and vertebral fractures in male osteoporosis. *J Bone Miner Res*. 2000; 15: 13-9.
39. Chen PY, Sun JS, Tsuang YH, Chen MH, Weng PW, Lin FH. Simvastatin promotes osteoblast viability and differentiation via Ras/Smad/Erk/BMP-2 signaling pathway. *Nutr Res*. 2010 ;30: 191-9.
40. Pauly S, Luttosch F, Morawski M, Haas NP, Schmidmaier G, Wildemann B. Simvastatin locally applied from a biodegradable coating of osteosynthetic implants improves fracture healing comparable to BMP-2 application. *Bone*. 2009; 45: 505-11.
41. Fromigue O, Hay E, Modrowski D, Bouvet S, Jacquel A, Auberger P. et al. RhoA GTPase inactivation by statins induces osteosarcoma cell apoptosis by inhibiting p42/p44-MAPKs-Bcl-2 signaling independently of BMP-2 and cell differentiation. *Cell Death Differ*. 2006; 13: 1845-56.
42. Quan H, He Y, Sun J, Yang W, Luo W, Dou C. Chemical self-assembly of multifunctional hydroxyapatite with a coral-like nanostructure for osteoporotic bone reconstruction. *ACS Appl Mater Interfaces*. 2018; 10: 25547-60.
43. Lv YJ, Yang Y, Sui BD, Hu CH, Zhao P, Liao L. et al. Resveratrol counteracts bone loss via mitofilin-mediated osteogenic improvement of mesenchymal stem cells in senescence-accelerated mice. *Theranostics*. 2018; 8: 2387.
44. Lin C, Yu S, Jin R, Xiao Y, Pan M, Pei F. et al. Circulating miR-338 Cluster activities on osteoblast differentiation: Potential Diagnostic and Therapeutic Targets for Postmenopausal Osteoporosis. *Theranostics*. 2019; 9: 3780.
45. Metavarayuth K, Maturavongsadit P, Chen X, Sitasuwan P, Lu L, Su J. et al. Nanotopographical cues mediate osteogenesis of stem cells on virus substrates through BMP-2 intermediate. *Nano Lett*. 2019; 19: 8372-80.